Journal of Thermal Analysis, Vol. 44 (1995) 937-954

DECARBONATION CURVES AND ASSOCIATED THERMODYNAMIC DATA FOR SYNTHETIC Cd-DOLOMITES $CdMg(CO_3)_2$, $CdMn(CO_3)_2$ AND $CdZn(CO_3)_2$

J. A. K. Tareen[1], *A. R. Fazeli*[1], *B. Basavalingu*[1] *and*
G. T. Bhandige[2]

[1]Department of Geology, University of Mysore, Mysore-570 006, India
[2]Department of Chemistry, Regional College of Education (NCERT) Mysore, India

(Received January 19, 1994; in revised form September 16, 1994)

Abstract

Decarbonation curve for the synthetic dolomite analogues; (Cd-dolomites) were determined for $CdMg(CO_3)_2$, $CdMn(CO_3)_2$ and $CdZn(CO_3)_2$ under CO_2 pressure of up to 2.5 kbar. All the three double carbonates were completely disordered at the decomposition temperatures and hence the thermodynamic data (Standard enthalpy; ΔH_f°, Standard free energy; ΔG_f°) retrieved from the univariant decarbonation curve corresponds to the disordered phases. They are:

	$CdMg(CO_3)_2$	$CdMn(CO_3)_2$	$CdZn(CO_3)_2$
ΔH_f° / kJ	-1863.5 ± 2.4	-1641.5 ± 3.0	-1566.3 ± 1.1
ΔG_f° / kJ	-1701.5 ± 2.4	-1490.0 ± 3.0	-1406.7 ± 1.1

The mixing enthalpies and free energies for the formation of the disordered 1:1 solid solution phases are:

	$CdMg(CO_3)_2$	$CdMn(CO_3)_2$	$CdZn(CO_3)_2$
$\Delta H^\circ_{(mix)}$ / J	+8.0	+11.6	+8.9
$\Delta G^\circ_{(mix)}$ / J	+4.9	+8.7	+5.8

The thermodynamic data (ΔH_f°, ΔG_f° and ΔH_r°, ΔG_r°) showed a positive correlation with the decomposition temperatures. The mixing energies of the disordered double carbonates also show a direct correlation with the cationic size differences.

Keywords: Cd-dolomites, decarbonation, synthetic dolomites, thermodynamic data

0368-4466/95/ $ 4.00

John Wiley & Sons, Limited
Chichester

Introduction

Studies pertaining to the synthesis, stability relations and cation ordering [1–3] of rhombohedral double carbonate, $CdMg(CO_3)_2$, a synthetic analogue of dolomite, $CaMg(CO_3)_2$, have been of interest to mineralogists because $CdMg(CO_3)_2$ shows much more defined and sharp ordering reflections in the X-ray diffractogram relative to dolomite, $CaMg(CO_3)_2$, or their equivalents such as kutnahorite, $CaMn(CO_3)_2$, or minrecordite, $CaZn(CO_3)_2$. Attempts to synthesize other transition metal dolomites $CaR^{2+}(CO_3)_2$ (where R=Fe, Co, Ni, Mn, Zn, Cu) in this laboratory and also by others were not successful except for $CaMn(CO_3)_2$ [4–7]. In this paper we report the results of such studies on the synthesis of $CdR^{2+}(CO_3)_2$ dolomite type double carbonates and on their equilibrium decomposition curves on the P–T plane. Thermodynamic data have also been derived for $CdMg(CO_3)_2$, $CdMn(CO_3)_2$ and $CdZn(CO_3)_2$ whose equilibrium decarbonation curves have been closely bracketed.

Experimental

All experiments were carried out with Tuttle type externally heated pressure reactors. The pressure medium was CO_2 gas which was pumped into the reactor before heating, using a pneumatic NOVA SWISS pressure pump. The solid charge was enclosed in crimped platinum tubes so that CO_2 had free communication with the charge. Details of this technique are given elsewhere [8, 9]. Two types of experiment have been carried out:

(a) runs for synthesis where the starting materials were mixtures of two carbonates in 1:1 ratio ($CdCO_3$ + $MgCO_3$, $CdCO_3$ + $MnCO_3$ etc.) and

(b) runs for construction of equilibrium decomposition curve wherein a three capsule technique was used. In this case, starting charges were 1) presynthesized double carbonate, 2) mixture of two carbonates in 1:1 ratio and 3) carbonate and an oxide with or without solid solution (e. g., $CdCO_3(ss)+ZnO(ss)$, $MgCO_3(ss)+CdO$, $MnCO_3+CdO$).

Trial synthesis runs were carried out starting with two carbonate mixtures $CdCO_3+MgCO_3$, $CdCO_3+MnCO_3$, $CdCO_3+FeCO_3$, $CdCO_3+CoCO_3$, $CdCO_3+NiCO_3$, $CdCO_3+ZnCO_3$. Table 1 gives the results of these runs at 1 kbar CO_2 pressure. A double carbonate $AB(CO_3)_2$ with nearly 1:1 ratio of A and B cations is stabilized with Cd–Mg, Cd–Mn and Cd–Zn combinations. In the rest, the products were only two carbonates with limited solid solubilities. Detailed studies were then carried out to construct the equilibrium decomposition curves for the double carbonates $CdMg(CO_3)_2$, $CdMn(CO_3)_2$ and $CdZn(CO_3)_2$. Starting materials using the three capsule technique mentioned above were used for these studies. The solid products after each run were iden-

Table 1 Hydrothermal runs for the synthesis of $CdR^{2+}(CO_3)_2$ (R=Mg, Mn, Fe, Co, Ni, Zn) at 1 kbar CO_2 pressure

$M'CO_3 + M''CO_3$	Temperature / °C	Duration / h	Solid product
$CdCO_3 + MgCO_3$	600	72	$CdMg(CO_3)_2$
$CdCO_3 + MnCO_3$	500	68	$CdMn(CO_3)_2$
$CdCO_3 + FeCO_3$	400	68	$CdCO_3$(ss) + Fe_3O_4
$CdCO_3 + FeCO_3$	300	68	$CdCO_3$(ss) + $FeCO_3$(ss) + Fe_2O_3
$CdCO_3 + CoCO_3$	400	84	$CdCO_3$(ss) + $CoCO_3$
$CdCO_3 + CoCO_3$	450	84	$CdCO_3$(ss) + $CoCO_3$
$CdCO_3 + NiCO_3$	300	72	$CdCO_3$(ss) + $NiCO_3$
$CdCO_3 + NiCO_3$	400	72	$CdCO_3$ + NiO
$CdCO_3 + ZnCO_3$	350	48	$CdZn(CO_3)_2$

tified using X-ray powder diffraction. When the experimental run was in a single carbonate field, the product in all the three capsules was a single phase of double carbonate. Likewise identical products were found in the field of decomposition. But, at the low temperatures the product of starting materials 2 and 3 was two carbonates, while the one starting with presynthesised double carbonate always remained unreacted with no sign of dissociation into two carbonates. The extent of solid solution in carbonates as well as oxides was estimated from the correlation of *d*-spacing with percent substitution, assuming that they have linear relation, as was found in case of Ca substitution in $MnCO_3$ and MnO [10].

Results

The experimental conditions and run products of the three double carbonates studied are provided in Tables 2–4, and the corresponding phase diagrams are given in Figs 1–3. Three fields of different phase assemblages are apparent from these diagrams. The low temperature region shows the formation of two carbonates while the double carbonate field falls in the middle, followed by decomposition separated by an univariant line. The field of two carbonates in low temperature region ("X" in Figs 1–3) was considered as metastable. This is because, we failed to dissociate a double carbonate (synthetic) into two carbonates, even with long runs of over 200 h. Even starting with the disordered $CdMg(CO_3)_2$ and $CdMn(CO_3)_2$ such a dissociation was not seen. Hence the low temperature two carbonate field was considered metastable. This is perhaps analogous to the first stage of dolomitization in nature, i.e. precipitation of disordered solid solution followed by dolomitization. Such an observation was also

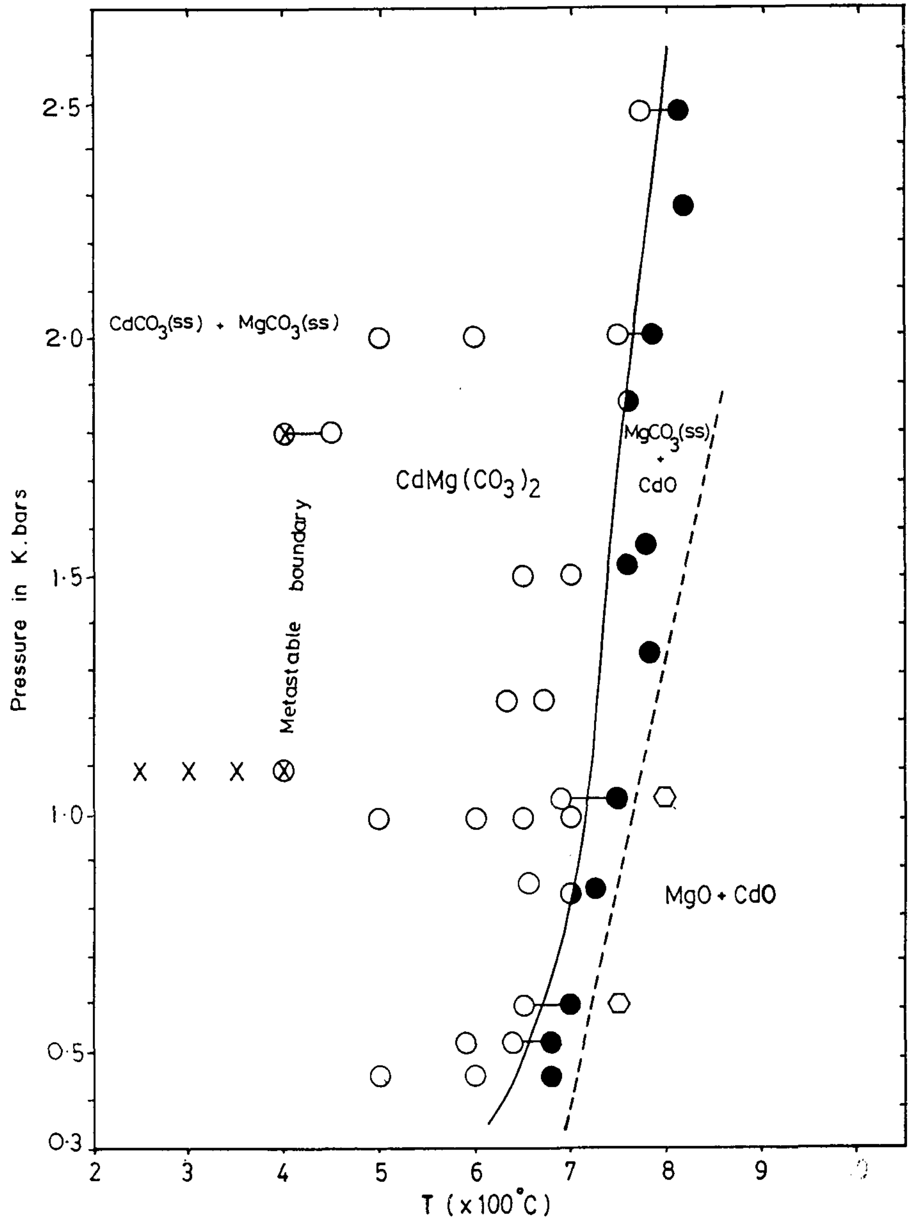

Fig. 1 *P–T* diagram for the decarbonation of $CdMg(CO_3)_2$. o = indicates formation of double carbonates; • = indicates decarbonation of double carbonates; x = indicates low temperature metastable carbonates

Table 2 Experimental details and run products in the system CdO–MgO–CO_2 at $X_{CO_2} = 0.1$. Starting materials $CdCO_3+MgCO_3$, $CdO+MgCO_3$ and $CdMg(CO_3)_2$ in three separate crimped capsules (Cd:Mg ratio 1:1)

Exp. No.	Temp. /°C	Press. / bar	Duration / h	Solid run products
418	590	520	48	$CdMg(CO_3)_2$
419	500	450	48	$CdMg(CO_3)_2$
423	600	450	48	$CdMg(CO_3)_2$
424	690	1034	48	$CdMg(CO_3)_2$
425	680	450	52	$MgCO_3$(ss) + CdO
426	630	1240	60	$CdMg(CO_3)_2$
427	670	1240	60	$CdMg(CO_3)_2$
428	820	2275	18	$MgCO_3$(ss) + CdO
429	780	1344	29	$MgCO_3$(ss) + CdO
433	780	1585	48	$MgCO_3$(ss) + CdO
434	750	1034	48	$MgCO_3$(ss) + CdO
435	775	2482	52	$CdMg(CO_3)_2$
460	800	1034	62	MgO + CdO
495	760	1516	60	$MgCO_3$(ss) + CdO
497	760	1860	62	$MgCO_3$(ss) + CdO
498	640	520	47	$CdMg(CO_3)_2$
499	680	520	47	$MgCO_3$(ss) + CdO
503	650	1500	60	$CdMg(CO_3)_2$
511	650	850	62	$CdMg(CO_3)_2$
512	725	850	62	$MgCO_3$(ss) + CdO
518	500	2000	62	$CdMg(CO_3)_2$
519	600	2000	62	$CdMg(CO_3)_2$
520	750	2000	60	$CdMg(CO_3)_2$
522	750	600	53	MgO + CdO
524	500	1000	77	$CdMg(CO_3)_2$
525	600	1000	77	$CdMg(CO_3)_2$
527	650	600	45	$CdMg(CO_3)_2$
528	700	600	120	$MgCO_3$(ss) + CdO
532	650	1000	45	$CdMg(CO_3)_2$
533	700	1000	45	$CdMg(CO_3)_2$
536	700	1500	65	$CdMg(CO_3)_2$
547	250	1100	200	$MgCO_3$(ss) + $CdCO_3$(ss)
548	300	1100	266	$MgCO_3$(ss) + $CdCO_3$(ss)
549	350	1100	200	$MgCO_3$(ss) + $CdCO_3$(ss)
550	400	1100	166	$CdMg(CO_3)_2$ + $MgCO_3$(ss) + $CdCO_3$(ss)

Table 2 Continued

Exp. No.	Temp. /°C	Press. / bar	Duration / h	Solid run products
557	400	1800	44	$CdMg(CO_3)_2$ + $MgCO_3$(ss) + $CdCO_3$(ss)
558	450	1800	44	$CdMg(CO_3)_2$
414	450	2480	48	$MgCO_3$(ss) + CdO
432	785	2000	48	$MgCO_3$(ss) + CdO
436	700	850	220	$CdMg(CO_3)_2$ + $MgCO_3$(ss) + CdO

Note: Two carbonates solid solution $CdCO_3$+$MgCO_3$(ss) in the low temperature region is metastable

Table 3 Experimental details and run products for hydrothermal decomposition of $CdMn(CO_3)_2$ in the system CdO–MnO–CO_2 at $X_{CO_2} = 0.1$. Starting material: $CdCO_3$+$MnCO_3$, CdO+$MnCO_3$ and $CdMn(CO_3)_2$ in three separate crimped capsules (Cd:Mn=1:1)

Exp. No.	Temp. /°C	Press. / bar	Duration / h	Solid run products
511	450	200	48	$CdMn(CO_3)_2$
553	525	200	56	$CdMn(CO_3)_2$
464	650	180	58	CdO + MnO
509	500	200	60	$CdMn(CO_3)_2$
471	625	140	70	CdO + MnO
484	500	520	66	$CdMn(CO_3)_2$
456	650	520	50	CdO + $MnCO_3$
462	650	620	150	CdO + $MnCO_3$
463	750	820	72	CdO + MnO
458	700	1035	48	CdO + $MnCO_3$
469	750	1035	58	CdO + MnO
457	600	1035	58	$CdMn(CO_3)_2$ + CdO + $MnCO_3$
486	650	1035	66	CdO + $MnCO_3$
550	400	1100	56	$CdMn(CO_3)_2$
505	575	850	66	$CdMn(CO_3)_2$
507	625	850	70	CdO + $MnCO_3$
467	800	820	70	CdO + MnO
547	250	1100	172	$CdCO_3$(ss) + $MnCO_3$(ss)
549	350	1100	150	$CdCO_3$(ss) + $MnCO_3$(ss)
508	400	1800	250	$CdCO_3$(ss) + $MnCO_3$(ss)
548	300	1100	258	$CdCO_3$(ss) + $MnCO_3$(ss)
449	400	1250	60	$CdMn(CO_3)_2$
450	500	1250	62	$CdMn(CO_3)_2$
473	700	1100	58	CdO + $MnCO_3$
476	550	1100	66	$CdMn(CO_3)_2$

Table 3 Continued

Exp. No.	Temp. /°C	Press. / bar	Duration / h	Solid run products
510	600	1400	68	$CdMn(CO_3)_2$
443	650	1450	70	$CdO + MnCO_3$
535	650	1500	70	$CdO + MnCO_3$
536	700	1500	48	$CdO + MnCO_3$
558	450	1800	58	$CdMn(CO_3)_2$
447	600	1860	64	$CdMn(CO_3)_2$
518	500	2000	66	$CdMn(CO_3)_2$
519	600	2000	66	$CdMn(CO_3)_2$
444	700	2060	56	$CdO + MnCO_3$
482	700	1250	58	$CdO + MnCO_3$
465	550	520	56	$CdMn(CO_3)_2$
455	600	520	62	$CdO + MnCO_3$
500	615	1300	56	$CdMn(CO_3)_2$
501	650	1300	58	$CdO + MnCO_3$
560	620	1650	62	$CdMn(CO_3)_2$
491	650	1650	58	$CdO + MnCO_3$
492	600	1100	62	$CdMn(CO_3)_2 + CdO + MnCO_3$
473	750	620	68	$CdO + MnO$
508	400	1800	50	$CdCO_3 + MnCO_3$

Note: The two carbonates $CdCO_3+MnCO_3$ in the low temperature region is metastable

Table 4 Experimental details and run products for hydrothermal decomposition of $CdZn(CO_3)_2$ in the system $CdO-ZnO-CO_2$ at $X_{CO_2} = 0.1$. Starting material: $CdCO_3+ZnCO_3$, $CdCO_3+ZnO$ and $CdZn(CO_3)_2$ in three separate crimped capsules (Cd:Zn = 1:1)

Exp. No.	Temp. /°C	Press. / bar	Duration / h	Solid run products
311	300	500	72	$CdZn(CO_3)_2$
316	350	1000	48	$CdZn(CO_3)_2$
335	450	2300	44	$CdZn(CO_3)_2$
591	400	1000	90	$CdZn(CO_3)_2$
326	500	2000	48	$CdCO_3$ + ZnO(ss)
334	550	2300	44	$CdCO_3$ + ZnO(ss)
312	450	500	76	$CdCO_3$ + ZnO(ss)
318	500	1500	62	$CdCO_3$ + ZnO(ss)
322	400	2000	48	$CdZn(CO_3)_2$
440	475	1000	85	$CdCO_3$ + ZnO(ss)
598	480	2000	48	$CdCO_3$ + ZnO(ss)

Table 4 Continued

Exp. No.	Temp. /°C	Press. / bar	Duration / h	Solid run products
599	450	2500	48	$CdZn(CO_3)_2$
439	550	980	85	$CdCO_3$ + ZnO(ss)
590	350	1500	90	$CdZn(CO_3)_2$
592	440	1000	90	$CdCO_3$ + ZnO(ss)
593	375	500	90	$CdZn(CO_3)_2$
594	400	500	90	$CdCO_3$ + ZnO(ss)
595	425	1500	48	$CdZn(CO_3)_2$
596	465	1500	48	$CdCO_3$ + ZnO(ss)
597	450	2000	48	$CdZn(CO_3)_2$
600	500	2500	48	$CdCO_3$ + ZnO(ss)
441	150	2000	85	$CdCO_3$ + $ZnCO_3$(ss)
444	200	2000	96	$CdCO_3$ + $ZnCO_3$(ss)
449	150	2300	100	$CdCO_3$ + $ZnCO_3$(ss)

Note: Two carbonates solid solution $CdCO_3+ZnCO_3$(ss) in the low temperature region is metastable

made by Katz and Mathews [11], for Mg-calcite equilibria in Mg-chloride solution under hydrothermal conditions and by Franke and Hofer [12] in $CaMn(CO_3)_2$ equilibrium studies. The authors have observed similar relations while studying the decomposition curves for $CaMg(CO_3)_2$ and $CaMn(CO_3)_2$ [9]. A schematic isobaric T–X diagram in the system $M'CO_3$–$M''CO_3$ is given in Fig. 4.

The first stage of high temperature decarbonation of the double carbonates was into an oxide and a carbonate. In the case of Cd–Mg and Cd–Mn carbonates the B-site cation, Mg and Mn form carbonates and CdO, while in Cd–Zn carbonate the A site cation, Cd forms carbonate and ZnO, with minor substitution of $Cd(Cd_xZn_{1-x}$ with average value of $x=0.15$).

$$CdMg(CO_3)_2 \rightarrow MgCO_3(ss) + CdO + CO_2$$

$$CdMn(CO_3)_2 \rightarrow MnCO_3 + CdO + CO_2$$

$$CdZn(CO_3)_2 \rightarrow CdCO_3(ss) + ZnO(ss) + CO_2$$

Thermodynamic data and discussion

Knowing the thermodynamic data for the phases on the product side of the equilibrium decomposition reaction in a P–T space (with well bracketed experimental P–T points for their univariant line) one can retrieve the standard en-

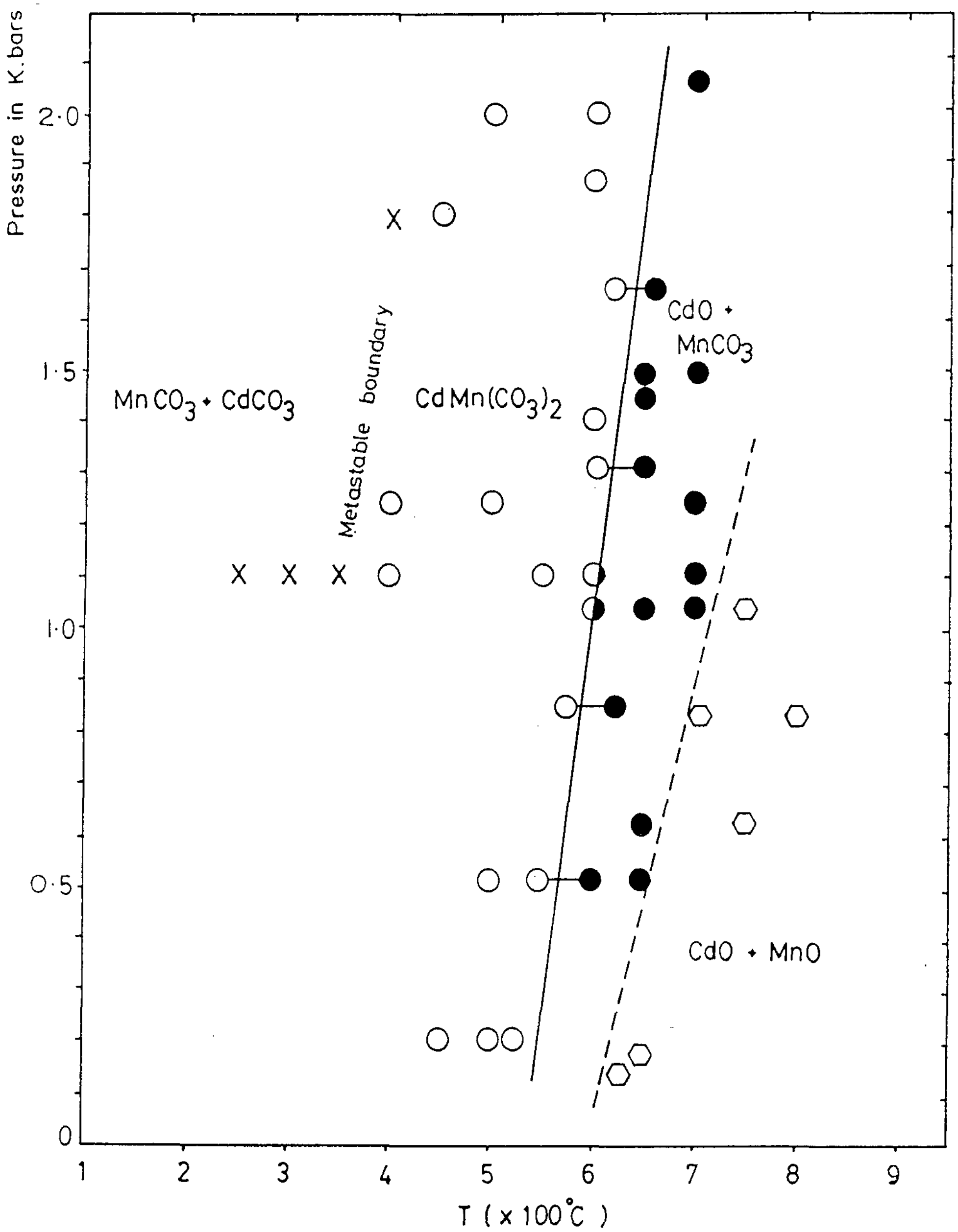

Fig. 2 *P–T* diagram for the decarbonation of CdMn(CO$_3$)$_2$. o = indicates formation of double carbonates, • = indicates decarbonation of double carbonates, x = indicates low temperature metastable carbonates

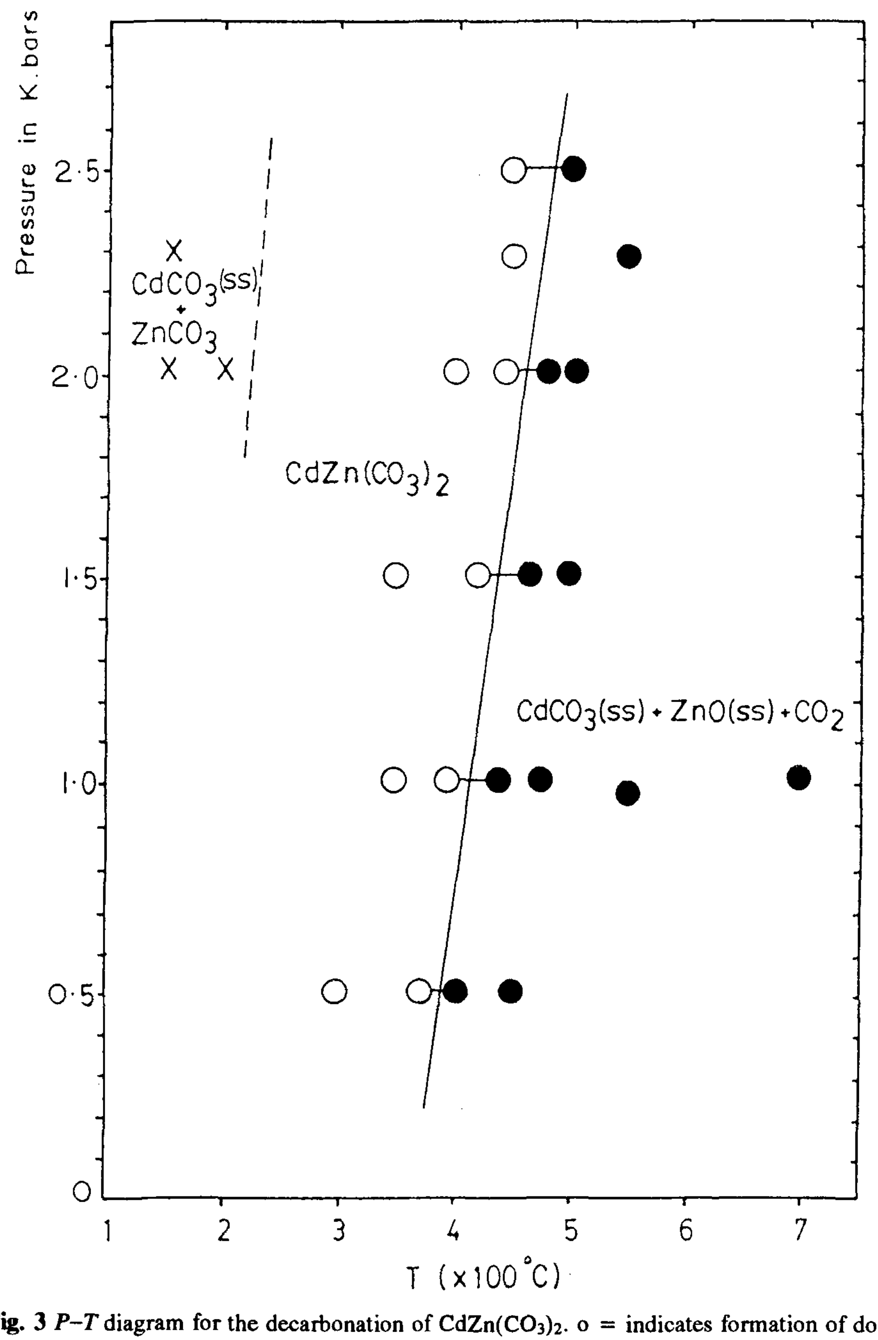

Fig. 3 *P–T* diagram for the decarbonation of $CdZn(CO_3)_2$. o = indicates formation of double carbonates, • = indicates decarbonation of double carbonates, x = indicates low temperature metastable carbonates

thalpy (ΔH°_f) and standard free energy (ΔG°_f) for these double carbonates from the expression,

$$\overset{AB(CO_3)_2}{\Delta H^\circ_{f(1,\,298)}} = \overset{ACO_3}{\Delta H^\circ_{f(1,\,298)}} + \overset{BO}{\Delta H^\circ_{f(1,\,298)}} + \overset{CO_2}{\Delta H^\circ_{f(1,\,298)}} + \Delta C_{p_r}(T_e - 298) - T_e[\Delta S^\circ_{r(1,\,298)} + \Delta C_{p_r} \ln (T_e/298)] + (P_e - 1)\Delta V^\circ_s + RT_e \ln fCO_2(P_e,\, T_e) \quad (1)$$

and

$$\Delta G^\circ_{r(1,\,298)} = \Delta H^\circ_{r(1,\,298)} - 298\Delta S^\circ_{r(1,\,298)} \quad (2)$$

where

$$\overset{AB(CO_3)_2}{\Delta G^\circ} = \Delta G^\circ_{r(1,\,298)} - \overset{Product}{\Delta G^\circ}$$

Here P_e and T_e refer to equilibrium pressure and temperature. The heat capacity change of the reaction (ΔC_{p_r}) was calculated by taking C_p of solids at 1, 298 (Table 5) and C_p for CO_2 was taken at P_e and T_e from Bottinga and Richet [13]. The fugacity of CO_2 was obtained from the program of Jacobs and Kerrick [14]. Since the entropy data for the double carbonates under consideration is not known, it was estimated by addition of reported entropy values of the

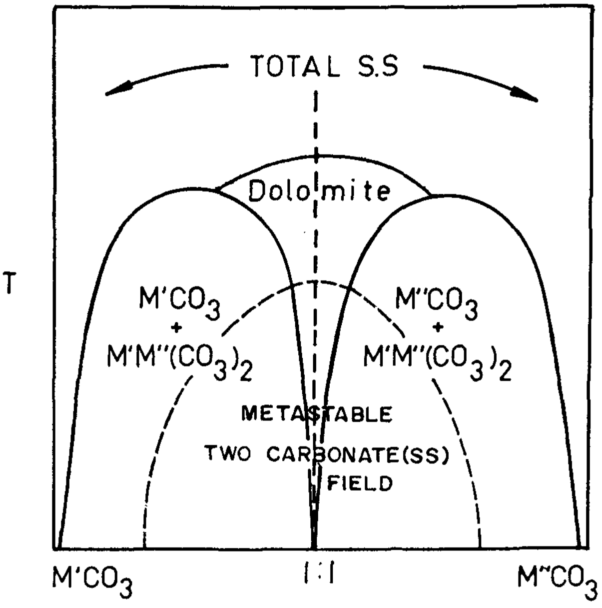

Fig. 4 Schematic isobaric *T–X* diagram showing the narrow stability field of dolomite type phase. The observed metastable field in Figs 1, 2 and 3 is also shown

end member carbonates together with a volume correction. The maximum entropy of the disordered double carbonates could be entropy of ordered + $2R$ ln 2, where the maximum disordering entropy would be 11.54 J·mol^{-1}·K^{-1}. The $\Delta S^{\circ}_{(1,298)}$ values were thus estimated considering double carbonates in the disordered state. The other reported thermodynamic data used in the present calculation are listed in Table 5 together with the sources. Table 6 gives the average

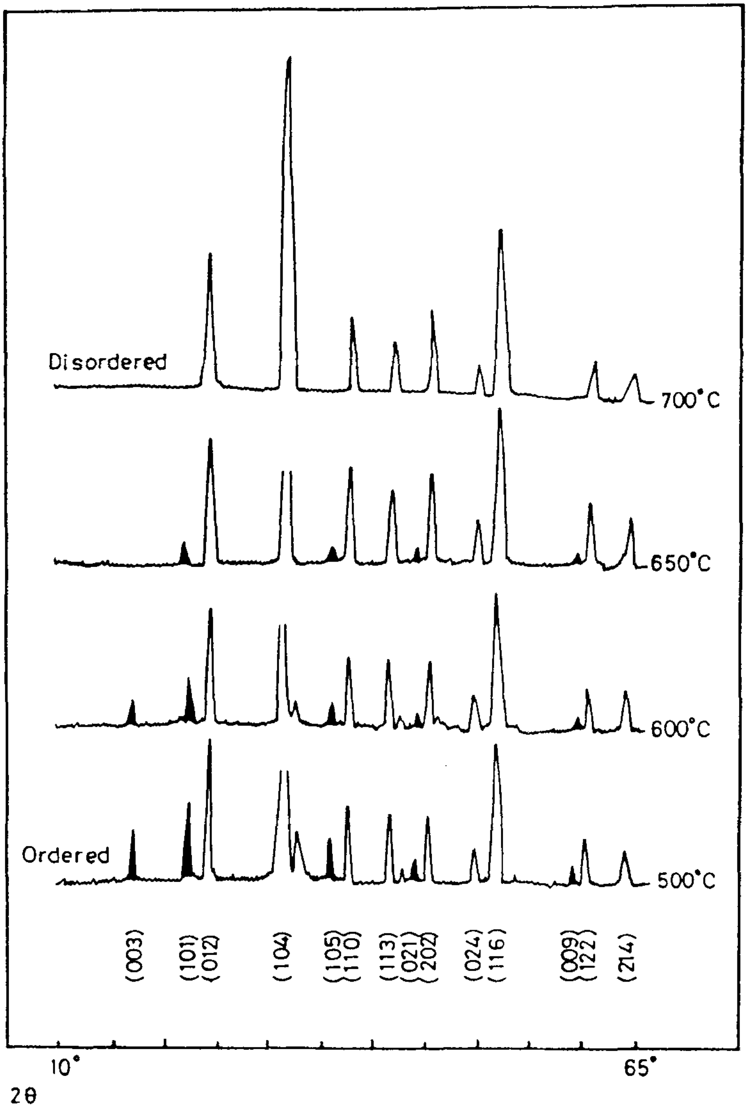

Fig. 5 Progressive disordering in $CdMg(CO_3)_2$ with increasing temperatures, visible from the intensities of characteristic X-ray reflections (shaded peaks)

Table 5 Reported thermodynamic data used in the calculation of standard enthalpy and free energy of double carbonates at $X_{CO_2} = 0.1$. (Entropy values given, for disordered double carbonates)

Compounds	ΔH_f° / kJ·mol^{-1}	ΔG_f° / kJ·mol^{-1}	S_f° / J·mol^{-1}·K^{-1}	Volume / cm^3	C_p° / J·mol^{-1}·K^{-1}
$CdMg(CO_3)_2$			167.8^{cal}	61.32^{cal}	167.3^k
$CdMn(CO_3)_2$			202.5^{cal}	64.34^{cal}	167.4^k
$CdZn(CO_3)_2$			184.9^{cal}	61.50^{cal}	167.3^k
$MgCO_3$	-1113.2*	-1029.5*	65.1*	28.01*	76.1*
$MgCO_3$ (ss)	-1106.2^{cor}	-1022.5^{cor}			
	- 889.3*	- 816.1*	100.0*	31.07*	75.5*
$MnCO_3$	- 891.9**	- 818.1**			
	-894.9^f	-821.8^f			
$CdCO_3$	-758.2^+	-676.9^+	92.5*	34.30*	83.5*
$CdCO_3$ (ss)	-761.1^{cor}	-679.8^{cor}			
ZnO	- 350.4*	- 320.5*	43.6*	14.33*	40.6*
ZnO(ss)	-336.6^{cor}	-306.7^{cor}			
CdO	- 258.2*	- 228.5*	54.8*	15.58*	42.5^k
CO_2	- 393.5*	- 394.4*	213.8*	–	++

Note:*) Robie *et al.*, [16], **) Robie *et al.*, [17], cor) Corrected value, cal) Calculated value, f) Fazeli *et al.*, [8], k) Knopp's rule, ++) New data from equilibrium decomposition curve of $CdCO_3$. +) C_p of CO_2 at P_e T_e from Bottinga & Richet [13]

Table 6 Average chemical composition of the solid decomposition products from d_{104}

Double carbonates	Solid decomposition products
$CdMg(CO_3)_2$	*CdO + $(Mg_{0.98}Cd_{0.02})CO_3$
$CdMn(CO_3)_2$	*CdO + $MnCO_3$
$CdZn(CO_3)_2$	$(Cd_{0.95}Zn_{0.05})CO_3$ + $Zn_{0.85}Cd_{0.15}O$

*Substitutions not detectable by X-ray powder diffraction

chemical composition of the solid products from X-ray spacings. As a result of this detectable solid solution it becomes necessary to suitably correct the reported ΔH_f° and ΔG_f° data of the solid solution phases before using them in the calculation. For instance:

$$\Delta H_f^\circ Cd_{0.95}Zn_{0.05}CO_3 = 0.95(\Delta H_f^\circ CdCO_3) + 0.05(\Delta H_f^\circ ZnCO_3) + \Delta H_{f(mix)}^\circ$$

The $\Delta H_{f(mix)}^\circ$ term can be ignored in view of the large enthalpy value and the corrected enthalpy data obtained. The same principle was applied for correcting ΔG_f° for the solid solution phases.

Table 7 Standard enthalpy and free energy data calculated, using the equilibrium decomposition curves for the rhombohedral double carbonates

$kJ\cdot mol^{-1}$	$CdMg(CO_3)_2$	$CdMn(CO_3)_2$	$CdZn(CO_3)_2$
ΔH_f^0	–1863.5±2.4	–1641.5±3.0	–1566.3±1.1
ΔG_f^0	–1701.5±2.4	–1490.0±3.0	–1406.7±1.1

Table 8 Mixing enthalpies and free energies computed for three double carbonates studied

$kJ\cdot mol^{-1}$	$CdMg(CO_3)_2$	$CdMn(CO_3)_2$	$CdZn(CO_3)_2$
$\Delta H_{(mix)}$	+7.9	+11.6	+8.9
$\Delta G_{(mix)}$	+4.9	+ 8.7	+5.8

It may be pointed out that the ordering reflections of dolomite were most easily visible in the diffractograms of $CdMg(CO_3)_2$, where they gradually decrease in intensity with increasing temperature (Fig. 5) and nearly disappear at the decomposition temperature. Hence the carbonate in equilibrium with its decomposition is considered to be fully disordered. The disordering temperature of Cd-dolomite was also studied by Goldsmith [1], who suggested its completion at 825°C. The other two carbonates $CdMn(CO_3)_2$ and $CdZn(CO_3)_2$ do not show ordering reflections at any of the temperatures studied. Besides, the disordering of $CaMn(CO_3)_2$, kutnahorite, was considered to begin at 400°C and be completed before the decomposition temperature by Goldsmith and Graf [15].

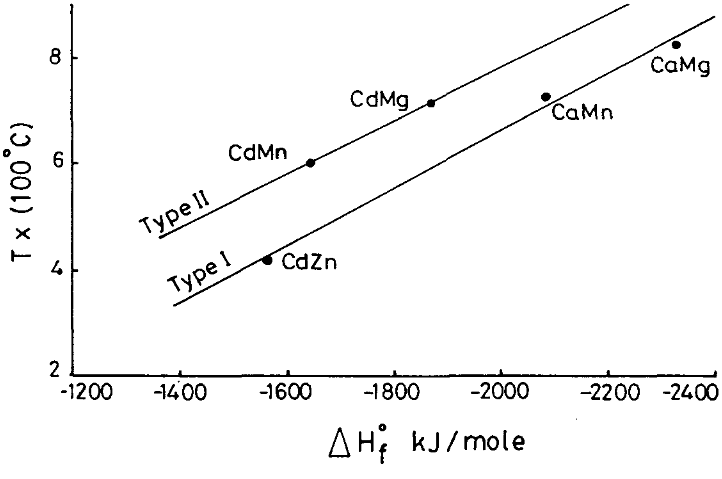

Fig. 6 Positive correlation between the increasing negativity of enthalpy of formation with that of the decarbonation temperatures at 1 kbar

Table 9 Decarbonation temperatures at 1 kbar CO_2 pressure for double carbonates

Compounds	Temperature / °C
$CaMg(CO_3)_2$	830
$CaMn(CO_3)_2$	730
$CdMg(CO_3)_2$	720
$CdMn(CO_3)_2$	610
$CdZn(CO_3)_2$	420

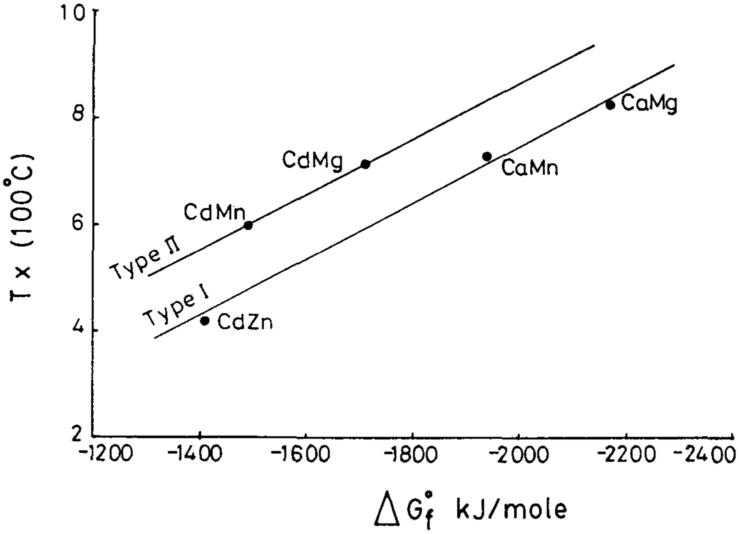

Fig. 7 Positive correlation between the increasing negativity of Gibbs free energy of formation with that of the decarbonation temperatures at 1 kbar

By analogy in the absence of ordering reflections, these double carbonates were also considered completely disordered at the equilibrium P–T points.

The standard ΔH_f^o and ΔG_f^o values for the disordered phases $CdMg(CO_3)_2$, $CdMn(CO_3)_2$ and $CdZn(CO_3)_2$ retrieved from these decarbonation curves are given in Table 7.

The ΔH_f (likewise ΔG_f) for a double carbonate can also be computed if the $\Delta H_{(mix)}$ is known through calorimetric determinations using the relation:

$$\overset{AB(CO_3)_2}{\Delta H_f^o} = \overset{ACO_3}{\Delta H_f^o} + \overset{BCO_3}{\Delta H_f^o} + \Delta H^o_{(mix)}$$

The $\Delta H^o_{(mix)}$ or $\Delta G^o_{(mix)}$ is negative if the double carbonate phase formed is ordered, and positive if the double carbonate is disordered. In the present case the positive $\Delta H^{\circ}_{f(\mathrm{mix})}$ value for the three disordered double carbonates obtained from the above reaction is given in Table 8.

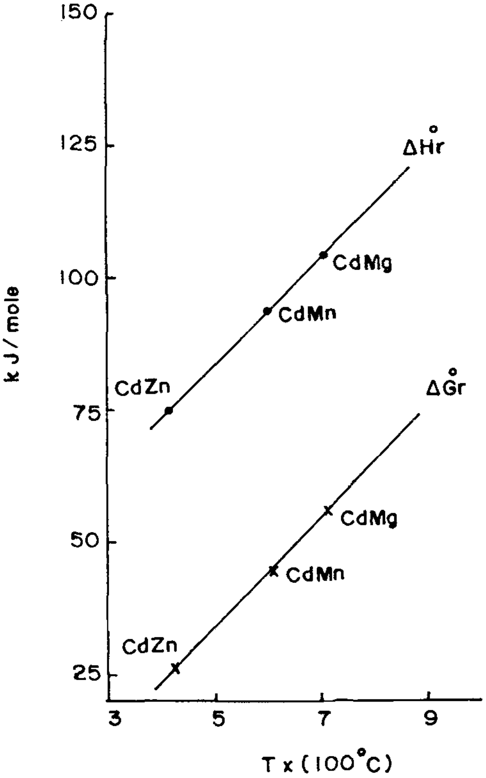

Fig. 8 Relationship between the decarbonation temperatures and the associated reaction free-energies and enthalpies

Of the three Cd-dolomites discussed here, only $CdMg(CO_3)_2$ was studied earlier using solution calorimetry by Capobianco *et al.*, [2], who measured the difference in the heat of solution of an ordered and disordered $CdMg(CO_3)_2$ to obtain the disordering enthalpy (13.7±0.8 kJ/mol). He also reported the enthalpy of formation of an ordered phase from $CdCO_3$ and $MgCO_3$ as −5.6±0.8 kJ/mol and +8.1±0.8 kJ/mol for the disordered phase. Our data for the enthalpy of formation of disordered $CdMg(CO_3)_2$ (+8.0 kJ/mol) compares well with the reported value of Capobianco. This strengthens the validity of our new thermodynamic data for the other disordered double carbonates $CdMn(CO_3)_2$ and $CdZn(CO_3)_2$, too.

In a similar study on $CaMg(CO_3)_2$ (dolomite) and $CaMn(CO_3)_2$ (kutnahorite) the authors have determined the ΔH°_{f} and ΔG°_{f} values. These values are also given in Table 7. The decomposition product in these carbonates was like

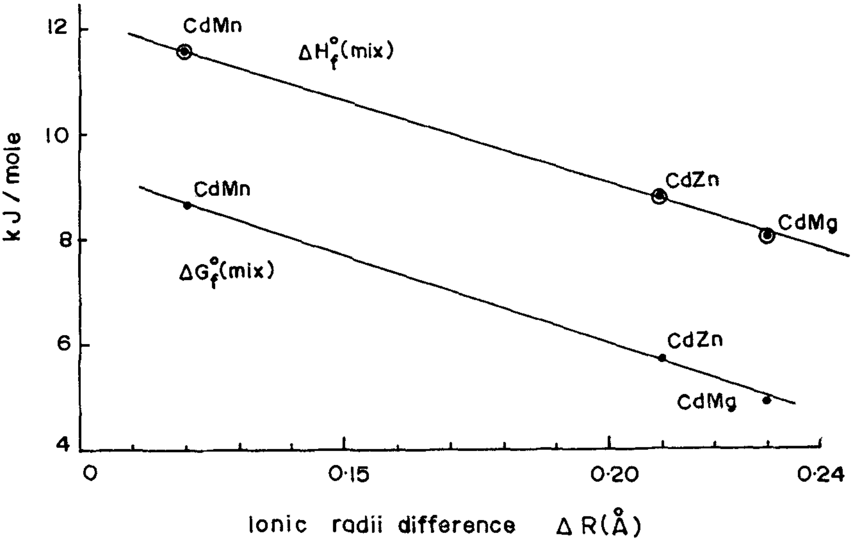

Fig. 9 Relationship between the ionic radii difference of A & B site cations and the mixing energies ($\Delta H^\circ_{f(mix)}$ and $\Delta G^\circ_{f(mix)}$) for disordered Cd-dolomites

the one in $CaZn(CO_3)_2$ with the A-site cation, Ca, forming the carbonate together with MgO or MnO as the case may be. Considering all the five double carbonates, we have two decomposition paths namely i) where the A-site cation come out as a carbonate (type I) and ii) where the B-site cation forms the carbonate. Since all these five double carbonates are isostructural and the thermodynamic data are available for them, an attempt was made to see if there is any correlation between the thermodynamic data and the decomposition temperatures. For the purpose of correlation the equilibrium decomposition temperatures at 1 kbar were taken for all the five double carbonates (Table 9).

A plot of both ΔH_f° and ΔG_f° data against the decomposition temperatures for the double carbonates, (Figs 6, 7) clearly shows a distinction between the carbonates of type I and type II decarbonation as discussed above. Besides a good positive correlation is seen between decarbonation temperatures and the electronegativity of both enthalpy and free energy values. The reaction enthalpy (ΔH_r°) and free energy (ΔG_r) also show a linear positive correlation with decomposition temperature (Fig. 8).

Another interesting correlation was between the mixing energies of the Cd-double carbonates and the ionic radii difference (ΔR) between the two cations in the A & B site of a dolomite (Fig. 9). The observed good correlation of the thermodynamic data with the decomposition temperatures and the cationic radii further confirms the reliability of the thermodynamic data on these isostructural double carbonates retrieved from univariant decarbonation phase boundary on the P–T plane.

The critical review of the manuscript by Dr. Eric J. Essene and Dr. G. M. Anderson is gratefully acknowledged.

References

1 J. R. Goldsmith, J. Geol., 80 (1972) 617.
2 C. Capobianco, B. P. Burton, P. M. Davidson and A. Navrotsky, J. Solid State Chem., 71 (1987) 214.
3 B. P. Burton, Am. Mineral., 72 (1987) 329.
4 P. E. Rosenberg, Am. J. Sci., 261 (1963a) 683.
5 P. E. Rosenberg and F. F. Foit, Geochim. Cosmochim. Acta, 43 (1979) 951.
6 J. R. Goldsmith, D. L. Graf, J. Witters and D. A. Northrop. J. Geol., 70 (1962) 659.
7 J. R. Goldsmith and D. Northrop, J. Geol., 73 (1965) 817.
8 A. R. Fazeli, J. A. K. Tareen, B. Basavalingu and G. T. Bhandage, Proc. Indian Acad. Sci., (Earth Planet. Sci.), 100 (1991) 37.
9 J. A. K. Tareen, A. R. Fazeli and B. Basavalingu, J. Geol. Soc. of India., 40 (1992) 545.
10 C. De Capitani and T. Peters, Contrib. Mineral. Petrol., 76 (1981) 394.
11 A. Katz and A. Mathews, Geochim. Cosmochim. Acta, 41 (1977) 297.
12 W. Franke and A. Hofer, Cryst. Res. Technol., 21 (1986) 1333.
13 Y. Bottinga and P. Richet, Am. J. Sci., 281 (1981) 615.
14 G. K. Jacobs and D. M. Kerrick, Computer and Geosciences, 7 (1981) 131.
15 J. R. Goldsmith and D. L. Graf, J. Geol., 68 (1960) 324.
16 R. A. Robie, B. S. Hemmingway and J. R. Fisher, U. S. Geol. Surv. Bull., 1452 (1978) 456.
17 R. A. Robie, H. T. Haselton and B. S. Hemmingway, Am. Mineral., 69 (1984) 349.

Zusammenfassung — Die Kurve für den Austrieb von CO_2 für synthetische Dolomitanaloge (Cd-Dolomite) wurde für $CdMg(CO_3)_2$, $CdMn(CO_3)_2$ und $CdZn(CO_3)_2$ bei einem CO_2-Druck bis zu 2.5 kbar ermittelt. Alle drei Doppelkarbonate werden bei den Zersetzungstemperaturen vollständig ungeordnet und folglich entsprechen die anhand der univarianten Dekarbonationskurve gewonnenen thermodynamischen Angaben (Standardenthalpie; ΔH°_f, Standard freie Energie; ΔG°_f) der ungeordneten Phase. Diese lauten:

	$CdMg(CO_3)_2$	$CdMn(CO_3)_2$	$CdZn(CO_3)_2$
ΔH°_f / kJ	-1863.5 ± 2.4	-1641.5 ± 3.0	-1566.3 ± 1.1
ΔG°_f / kJ	-1701.5 ± 2.4	-1490.0 ± 3.0	-1406.7 ± 1.1

Die Mischungsenthalpien und freien Energien für die Bildung der ungeordneten 1:1 Mischkristallphase lauten:

	$CdMg(CO_3)_2$	$CdMn(CO_3)_2$	$CdZn(CO_3)_2$
$\Delta H^\circ_{(mix)}$ / J	+8.0	+11.6	+8.9
$\Delta G^\circ_{(mix)}$ / J	+4.9	+8.7	+5.8

Die thermodynamischen Daten (ΔH°_f, ΔG°_f und ΔH°_r, ΔG°_r)) zeigen eine positive Korrelation mit den Zersetzungstemperaturen. Die Mischungsenergien der ungeordneten Doppelkarbonate zeigen auch eine direkte Korrelation mit den Unterschieden der Kationengröße.